

Late Holocene geochemical signature of inter reef mixed sediments on the northeastern Brazilian outer shelf

Assinatura Geoquímica do Holoceno tardio em sedimentos mistos inter-recifais na plataforma externa do nordeste do Brasil

Luzia Liniane do Nascimento Silva^{ab} , Moab Praxedes Gomes^{ac} , Patrícia Pinheiro Beck Eichler^{ad} , Helenice Vital^{ae} 

^aPrograma de Pós-Graduação em Geodinâmica e Geofísica, Universidade Federal do Rio Grande do Norte

^bluzialiniane@gmail.com, ^cmoab.gomes@ufrn.br, ^dpatriciaeichler@gmail.com, ^ehelenice.vital@ufrn.br



© 2024 The authors. This is an open access article distributed under the terms of the Creative Commons license.

Abstract

The northeastern outer shelf in Brazil is a complex ecotone that holds significant information on Holocene sedimentary processes and evolution. X-ray diffraction (XRD), X-ray fluorescence (XRF), and scanning electron microscopy/energy dispersive spectrometry (SEM/EDS) were employed to investigate bioclastic sedimentary facies and patches of relict siliciclastic sands. Radiocarbon dating (AMS) indicates that the carbonate sediments and corals formed in the past millennium. The sediment samples were divided into two groups using a multivariate analysis of XRD and XRF. The first group consists of siliciclastic materials, characterized by Si, Al, Fe, K, Zr, and Ti, and has low levels of carbonate and organic matter. The second, bioclastic and mixed facies, has a high carbonate content and exhibits elevated concentrations of Ca, Sr, and Mg, indicating authigenic processes. The EDS data revealed that the shells predominantly consisted of Cl, Cu, Al, Fe, and Ca. The terrigenous sites are detached from the coastal sources and are mainly located within the reef areas of the outer shelf. The erosion processes in these areas were inefficient to eliminate the siliciclastic sediments. This deposit trapped in inter reef sediments holds the key to understanding the timing and interactions between past coastal processes, shelf valley incision, and reef evolution during the Late Holocene transgression.

Keywords: Siliciclastic facies, heavy minerals, radiocarbon dating, reefs, marine sediments.

Resumo

A plataforma externa nordeste do Brasil é um ecótono complexo que contém informações significativas sobre os processos sedimentares e sua evolução do Holoceno. Difração de raios X (DRX), fluorescência de raios X (XRF) e microscopia eletrônica de varredura/espectrometria de energia dispersiva (SEM/EDS) foram empregadas para investigar fácies sedimentares bioclásticas e manchas reliquias de areias siliciclásticas. Datações por radiocarbono (AMS) revelaram que os sedimentos carbonáticos e os corais se formaram no último milênio. Utilizando uma análise multivariada de DRX e FRX, as amostras de sedimentos foram divididas em dois grupos. O primeiro grupo é composto por sedimentos siliciclásticos, caracterizados por Si, Al, Fe, K, Zr e Ti, e apresenta baixos teores de carbonato e matéria orgânica. O segundo grupo, fácies bioclástica e mista, possui alto teor de carbonatos com concentrações elevadas de Ca, Sr e Mg, indicando processos autigênicos. Os dados EDS mostraram que as conchas consistiam predominantemente de Cl, Cu, Al, Fe e Ca. Os resultados indicam que os sítios terrígenos estão separados das fontes costeiras e estão localizados principalmente nas áreas dos recifes da plataforma externa. Os processos erosivos nessas áreas foram ineficientes na eliminação dos sedimentos siliciclásticos. Este depósito confinado entre recifes é a chave para a compreensão da cronologia e das interações entre os processos costeiros passados, a incisão do vale da plataforma e a evolução dos recifes durante a transgressão do Holoceno tardio.

Palavras-chave: Fácies siliciclásticas, minerais pesados, datação radiocarbono, recifes, sedimentos marinhos.

1. Introduction

Textural characteristics and chemical composition of sediments record diagenetic changes in siliciclastic and carbonate facies (Sevastjanova et al. 2012, Nisha & Achyuthan 2014, Almeida et al. 2017). Numerous studies have been conducted on sedimentary provenance to reconstruct erosion and deposition processes, employing methods like isotopic analysis,

geochemistry, petrography, heavy mineral analysis, and statistics (Arz et al. 1998, Sevastjanova et al. 2012, Wu et al. 2017, Nascimento Silva & Gomes, 2019). Nevertheless, paleoenvironmental studies have certain limitations, including the poor preservation of transgressive deposits on continental shelves (Cattaneo & Steel, 2003, Gonzalez et al. 2004), accurate dating, and robust proxy records, which are essential

prerequisites for reconstructing paleoenvironments (Gao et al. 2019).

The understanding of shelf sedimentation provides valuable insights into the mechanisms of transport, hydrodynamic regimes, morpho-sedimentary features of the shelf, and lithology of the adjacent land areas (Nisha & Achyuthan 2014, Bastos et al. 2015). For instance, sedimentary processes during low relative sea level and the subsequent transgression determine the supply rates and spatial distribution of terrigenous sediment. In comparison, the production of carbonate sediments is primarily driven by biological activity, such as the formation and degradation processes of shells and skeletons (Tucker 1985, Gischler 2011, Bosence 2021). Thus, the occurrence of these two sedimentary facies depends on different processes, and the rise of siliciclastic sediment might lead to a decline in carbonate production. The drowning of shelves and the landward migration of coastal systems leave relict sedimentary deposits in deeper parts of shelves with no relation to their pristine environments (Emery 1968, Mount 1984).

Modern sedimentation in starved mixed carbonate-siliciclastic shelves often preserves the trapping and reworking of relict sand sheets into near-shore and shelf sand-ridges, reefs, and valleys (Miller et al. 2014). Abrupt changes in sediment facies, influenced by paleotopography and hydrodynamics, can reveal the simultaneous occurrence of modern and relict sediments. As an example, sediment records from the Turkey shelf indicate a decline in the land-derived sediment accumulation since the Late Holocene. This led to modern sediments being limited to the inner shelf, with relicts found in deeper shelf areas (Alavi et al. 1989). Another example is in the Gulf of Papua (Pandora Trough), the siliciclastic sediments were completely removed or buried during the melting water pulse 1B, while calciturbidite developed after the subsequent flooding of the Eastern Fields Reef (Jorry et al. 2008).

In the continental shelf of northeastern Brazil, transgressive and regressive events interfinger carbonate and siliciclastic sediments since the Miocene (Pessoa Neto 2003). Since last deglaciation, the sediment-starved shelf in a semi-arid climate has been characterized by limited estuaries and tidal channels (Barbosa et al. 2018, Ferreira et al. 2022). In this scenario, the preservation of sedimentary deposits is difficult due to the erosional context, which spreads carbonate and siliciclastic facies along and across-shelf (Nascimento Silva et al. 2018, Vieira et al. 2019, Morais et al. 2020). Nonetheless, if shelf inundation occurs rapidly, sea-level indicators like terraces, reefs, and incised valleys are more probable to be preserved (Camargo et al. 2015, Gomes et al. 2020, Morais et al. 2020). However, this could lead to the formation of shelf deposits that are limited to certain zones, where coralline algae gather on the outer shelf and quartz sands are found mainly in shallower water depths (Vital

et al. 2008, Dominguez et al. 2013, Moreira et al. 2020).

This present study aimed to investigate the sources and controls involving mixed siliciclastic and carbonate sediments found on the outer shelf of the Rio Grande do Norte (RN), northeastern Brazil (Fig. 1). Geochemical analysis (XFR, XRD, and MEV/EDS) were applied to identify the processes on sediment deposition and the main factors controlling their distribution patterns. Additionally, AMS radiocarbon dating was employed to examine the sedimentation events and analyze the sedimentary evolution during the Holocene.

2. Regional settings

The study area is the outer continental shelf of RN (Figs. 1 and 2). This is clearly compartmentalized in the inner shelf, between coastline and 25 m water depth, and outer shelf, between 25 and the shelf break at approximately 70 m (Gomes et al. 2020). A middle environment occurs locally near the Açú Incised Valley (Gomes et al. 2014, 2015). The continental shelf presents distinct physiography in their compartments with a very low gradient (1:1500) on the inner shelf and a steeper gradient (1:200) on the outer shelf (Gomes & Vital 2010, Gomes et al. 2014, 2015). The shelf presents mixed carbonate-siliciclastic sedimentation, with the shallow portion being siliciclastic, the intermediate is siliciclastic and carbonate and the outer region is predominantly carbonate, which are sensitive to climatic changes and hydrodynamic regimes (Vital et al. 2008, Gomes et al. 2015, 2016, Nascimento Silva & Gomes 2019).

In the outer shelf, along approximately 60 km over terraces between 25 and 45 m water depths, the reef field Açú Reefs is composed of patches of knolls and ridges with an average height of 4 m, which geomorphological evidence shows that the latest reef generation were formed after 11 kyrs BP (Nascimento Silva et al. 2018, Nascimento Silva & Gomes 2019, Gomes et al. 2020), spanning from the end of the Younger Dryas, and through millennial events of sea-level rise until sea level reached the current position since 7 kyr (Bezerra et al. 2003, Stattegger et al. 2006, Nascimento Silva et al. 2018, Angulo et al. 2022). Laterally, marine terraces occur on the northern and eastern outer shelf of the RN at depths below 25 m (Gomes et al. 2020). Subaqueous dunes have also been identified on the transition between the inner and outer compartments (Vital et al. 2008, Nascimento Neto et al. 2019). The Açú Incised Valley cut the entire shelf and left a Pleistocene morphological expression on the modern shelf surface (Vital et al. 2010a, 2010b, Schwarzer et al. 2006, Gomes et al. 2014, 2015, 2016). It is an important morphological barrier for the easterly shelf sediment migration with a narrower shape, with a maximum width of 2 km on the middle and outer shelf (Gomes & Vital 2010, Gomes et al. 2014). This negative relief of the valley, of about 20 m, channelizes tidal currents and induces a complex process of

sediment mixing (Gomes et al. 2016). At the shelf edge, submarine canyons have widths of up to 6 km (Almeida et al. 2015). They are also important structures for sediment transference, which become very active during the lower sea levels, when river runoff erosive processes intensify in the shelf break, whereas gravity flows, ocean forces, and tectonic activity rejuvenate the slope features (Almeida et al., 2015).

The continental shelf of RN is characterized as a complex high-energy system formed by the combination of winds, waves, tides, and ocean currents

(Testa & Bosence 1999, Vital 2009, Vital et al. 2010a, Gomes et al. 2016). Wave and tide processes have a constant influence on coastal dynamics, with the tidal ranges of 3.3 m in the spring tidal and 1.2 m in the neap tidal and with the wave height maximum is 80 cm and the minimum is 22 cm in the breaker zone (Lima & Vital 2006, Vital 2009, Vital et al. 2010a). The North Brazil Current streams the shelf with parallel flow parallel to the coast with speeds of 30-40 cm/s (Knoppers et al. 1999). On the mid-and outer shelf, the dominant easterly tide-wind-driven currents have an average speed of 24 cm/s (Gomes et al. 2016).

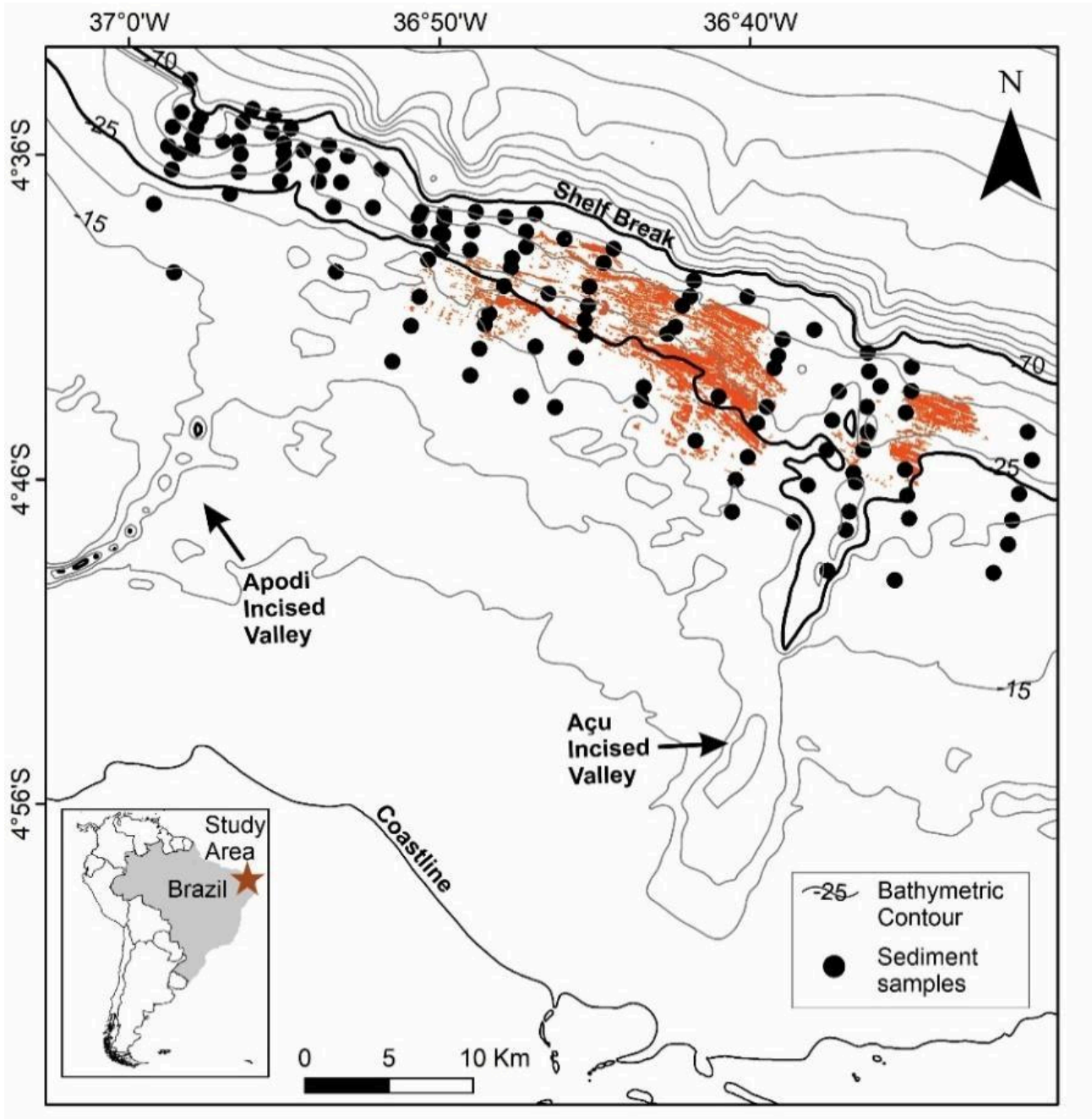


Figure 1 - Bathymetric map of northern RN shelf with sites of sediment samples and main shelf features and indication of the Açú Reefs in orange shapes (after Nascimento Silva et al. 2018).

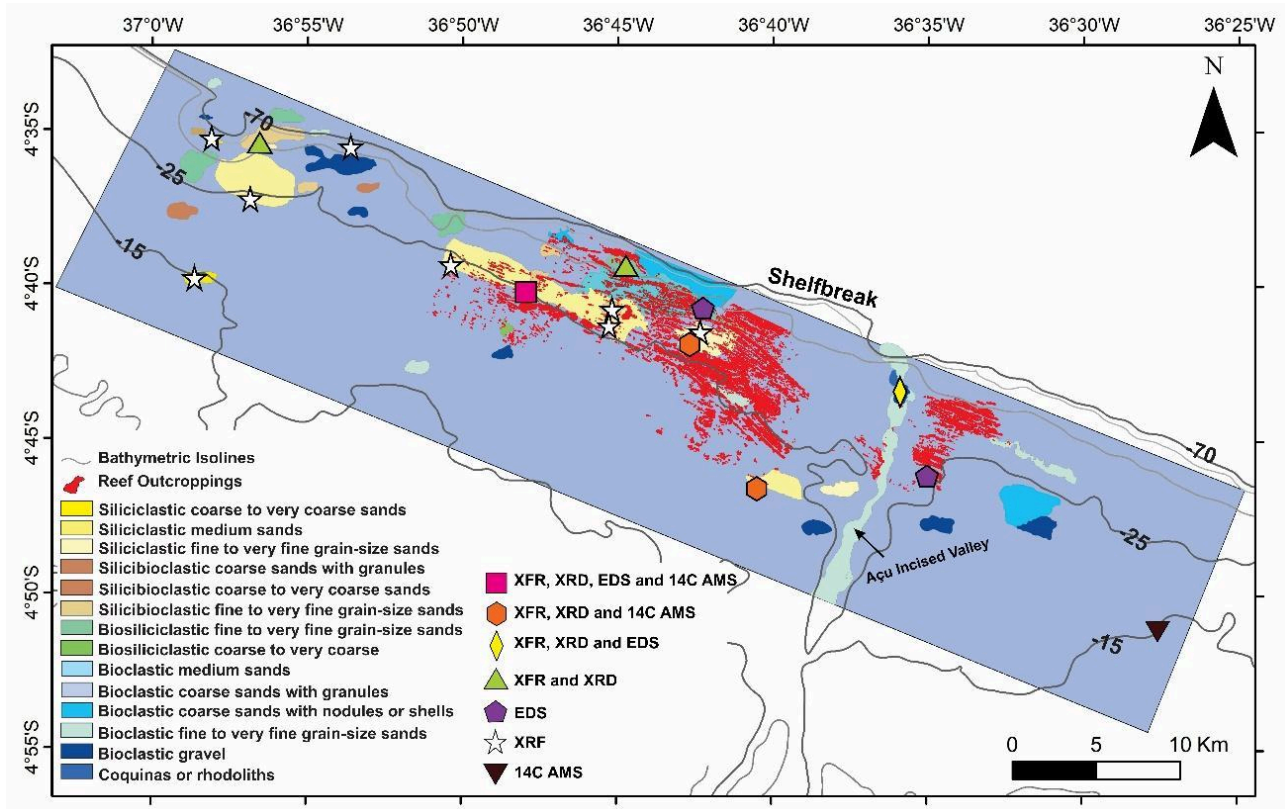


Figure 2 - Study area map showing the outer continental shelf with the distribution of the sediment samples used to XRD, XRF, EDS, and radiocarbon dating (AMS) analyzes. Sedimentological map including the Açú Reef distribution are after Nascimento Silva et al. (2018).

3. Materials and methods

A total of 123 sediment samples were collected along transects of 10 km perpendicular to the shelf edge with a distance of approximately 2 km between samples (Fig. 2). The survey was carried out in June 2015 and June 2016 using the Van Veen grab sampler with which support and positioning system (Datum WGS - 84) of the hydrographic ship of the Brazilian Navy Balizador Manhães H20 (Nascimento Silva et al. 2018, Nascimento Silva & Gomes, 2019). Grain size analysis follows the procedure of samples washing three times to remove salts, drying at 50 °C oven-dried, homogenization, and splitting. The subsamples were separated by weighing ~10 g for quantification of calcium carbonate via 10% HCl attack, measuring the initial and final weights, which provided the carbonate content. Another ~10 g of each sample was subject to weight loss on ignition (LOI) by weighing the samples after drying at 600 °C for organic matter incineration.

Grain size patterns were analyzed following Folk (1974). Leptokurtic distributions indicate uniform, hydrodynamically compatible grain sizes, likely due to prolonged transport or reworking. Mesokurtic distributions show intermediate patterns, while platykurtic distributions reflect a wide range of particle sizes, attributed to varying sedimentation processes or sources (Nascimento Silva & Gomes 2019). The sedimentary facies classification proposed by SAG software (Dias & Ferraz 2004) and adapted to local

classes based on Vital et al. (2008) (after Larsonneur 1977).

Geochemical analysis took the sediments passed through a 230-mesh sieve. The X-ray diffraction analysis (XRD) used ~ 5g from 18 samples and the X-ray fluorescence (XRF) analysis used ~ 5g from 14 samples. Based on sample site and compositions, 10 samples were used for scanning electron microscopy/energy dispersive spectrometry (SEM/EDS) analysis. The XRD analysis of samples were performed using a D8 ADVANCE Eco, with KCu α emission scanning of 2° to 55°, under a scan speed of 2°/min. The concentration of chemical elements was determined by XRF with a Shimadzu EDX 720 diffractometer equipped with Rh tube. Particles of different samples (i.e., 55, 70, and 130) were selected by binocular analysis and were adhered to two-sided carbon adhesive tape over an Al support. The morphological data and x-ray microanalysis results used a scanning electron microscope (FEI/Philips XL30 FEG ESEM) with Electron Backscatter Diffraction analysis and Energy-Dispersive X-ray operating in a high-vacuum mode with an acceleration voltage of 20 kV, 50 s of acquisition time, and a 35° elevation.

The multivariate analysis was applied to the interpretation of the metals distribution in the sediments, using the unweighted pair-group mean average (UPGMA) algorithm, following the calculation of the Euclidean distance between samples, and also

Principal Components Analysis (PCA) was applied to observe distinct behavior of the variables metals, carbonate content, and organic matter. The numerical procedures of the analysis were carried out using PAST (Hammer et al. 2001), the dataset was normalized and transformed in a similarity matrix and the correlations were tested for significance in statistical parameters where $\alpha < 0.05$ provided a significant correlation.

Additionally, the ¹⁴C ages of four sediment samples with carbonate content where siliciclastics

dominate and two corals (*Siderastrea* sp.) were determined using accelerator mass spectrometry (AMS), at the Poznań Radiocarbon Laboratory, Poland. The calibration was made with the OxCal v4.4.2 software (Bronk Ramsey 2009) using marine data from Heaton et al (2020). The results of calibration are given in intervals of calendar age with the probability of ca. 68% and ca. 95%. Uncalibrated and calibrated ages are shown in Table 1.

Table 1 – Uncalibrated and calibrated (AMS) radiocarbon ages.

Lab. Number/ Samples	Depth (m)	Conventional Ages C14 and Uncertainty	1-Sigma 68.3% probability	2-Sigma 95.4% probability	Years before 1950 yr BP (cal. BP)		Age BP (mean probability)
					(max)	(min)	
Poz-118053/ AcuCoral02	25	840 +/-30	1464-1676 AD	1380-1838 AD	570	112	341
Poz-118054/ AcuCoral03	17	435 +/-30	1853 AD	1907 AD	97	43	70
Poz-118061/ AcuSed01(AR-71)	30	715 +/-30	1565-1819 AD	1497-1942 AD	453	8	231
Poz-118060/ AcuSed02 (AR-55)	30	890 +/-30	1437-1645 AD	1323-1770 AD	627	180	404
Poz-118058/ AcuSed03(AR-46)	25	935 +/-30	1402-1617 AD	1290-1710 AD	660	240	450
Poz-118005/ TubSed01	15	900 +/-30	1430-1640 AD	1315-1756 AD	635	194	415

4. Results

4.1 Sedimentary analysis

The siliciclastic sands are predominantly medium sand grain size (1 - 2 ϕ), moderately sorted, symmetrical, and mesokurtic. The bioclastic sediments are very fine gravel (-1 - 2 ϕ), poorly sorted, very fine skewed, and platykurtic. The mixed sediments are fine grain-size (2 - 3 ϕ), poorly sorted, very coarse skewed, and mesokurtic to very leptokurtic. The CaCO₃ content of the sediments ranges from 3 to 99% and the organic matter ranges from 0 to 5% (Table 2). The bioclastic facies consist of fragments of benthic foraminifera, bivalves, gastropods, ostracods, molluscs, and Halimeda (Fig. 3).

To identify the minerals in the sedimentary facies of the shelf, especially the siliciclastic ones, XRD analyses were employed. The mineralogical analysis of the selected samples revealed that the sediments mainly consist of calcite, aragonite, and quartz. The most significant calcite concentrations were discovered in samples 17, 46, 55, 71, and 78 (Fig. 4a), with sample 17 being the most consistent and located in the AIV at a water depth of 40 m. The presence of aragonite is restricted to sample 78, occurring as a secondary mineral beneath quartz at 45 m water depth. Quartz was found in samples 55, 78, and 130. Staurolite is present in samples 55 and 71, strontianite and zircon are found in sample 78, and sample 130, near the head of the canyons at a water depth of 55 m (Fig. 4f), contains wollastonite and zoisite.

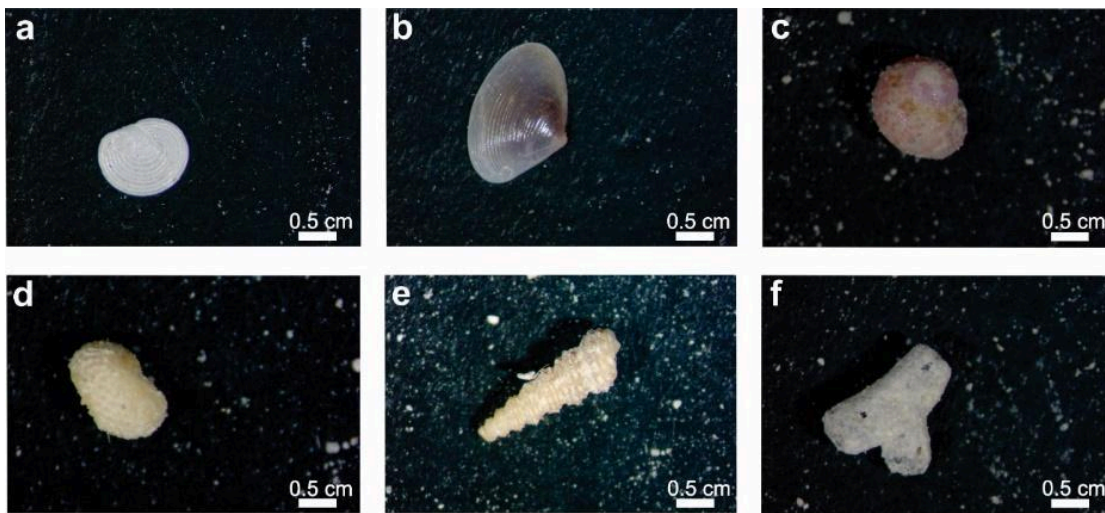


Figure 3 - Biogenic constituents. a) benthic foraminifera; b) bivalves; c) gastropods; d) ostracods; e) molluscs, and f) Halimeda.

Table 2 - Sedimentary facies types of sediment samples.

Sediment Samples	Sedimentary facies	Depth (m)	Carbonate (%)	Organic matter (%)	Mean	Sorting	Skewness	Kurtosis	Statistical Classifications
17	Bioclastic gravel	40	99.6583	5.6700	1.600	1.861	-0.396	0.798	Very Fine Gravel, Poorly Sorted, Very Fine Skewed, Platykurtic
34	Bioclastic coarse sands with granules	25	98.4312	7.4400	-0.408	1.362	0.412	0.933	Very Coarse Sand, Poorly sorted, Very Fine Skewed, Mesokurtic
46	Siliciclastic medium sands	25	20.3790	2.4700	1.839	1.015	-0.102	1.288	Medium Sand, Poorly Sorted, Symmetrical, Leptokurtic
55	Siliciclastic medium sands	30	3.8378	1.2000	1.234	0.761	-0.083	1.036	Medium Sand, Moderately Sorted, Symmetrical, Mesokurtic
69	Biosiliciclastic fine to very fine grain-size sands	37	65.5711	4.5400	2.239	1.054	-0.032	0.932	Fine Sand, Poorly Sorted, Symmetrical, Mesokurtic
70	Siliciclastic fine to very fine grain-size sands	35	29.2157	2.9800	2.302	1.384	-0.392	2.209	Fine Sand, Poorly Sorted, Very Coarse Skewed, Very Leptokurtic
71	Siliciclastic fine to very fine grain-size sands	30	18.3676	2.1000	2.360	1.381	-0.394	2.397	Fine Sand, Poorly Sorted, Very Coarse Skewed, Very Leptokurtic
78	Biosiliciclastic fine to very fine grain-size sands	45	51.4001	3,7900	2.567	1.501	-0.609	1.009	Fine Sand, Poorly Sorted, Very Coarse Skewed, Mesokurtic
80	Silicibioclastic fine to very fine grain-size sands	30	35.4315	3.7400	2.461	1.080	-0.300	2.572	Fine Sand, Poorly Sorted, Fine Skewed, Very Leptokurtic
81	Siliciclastic medium sands	25	14.2971	1.2700	1.828	0.817	-0.025	0.930	Medium Sand, Moderately Sorted, Symmetrical, Mesokurtic
90	Siliciclastic medium sands	25	3.9144	0.9400	1.259	0.715	-0.116	1.107	Medium Sand, Moderately Sorted, Coarse Skewed, Mesokurtic
114	Siliciclastic coarse to very coarse sands	40	19.2150	2.1902	1.418	1.68	-0.108	0.841	Medium Sand, Poorly Sorted, Symmetrical, Platykurtic
128	Siliciclastic medium sands	25	1.5118	0.6825	1.418	1.168	-0.108	0.841	Medium Sand, Poorly Sorted, Coarse Skewed, Platykurtic
130	Siliciclastic fine to very fine grain-size sands	55	5.9604	0.7933	2.197	0.632	-0.249	0.883	Fine Sand, Moderately Well Sorted, Coarse Skewed, Platykurtic
138	Siliciclastic coarse to very coarse sands	20	5.2588	0.3614	0.887	0.630	0.159	0.769	Coarse Sand, Moderately Well Sorted, Fine Skewed, Platykurtic
162	Siliciclastic medium sands	95	24.8685	1.4886	1.824	0.774	0.086	1.088	Medium Sand, Moderately Sorted, Symmetrical, Mesokurtic

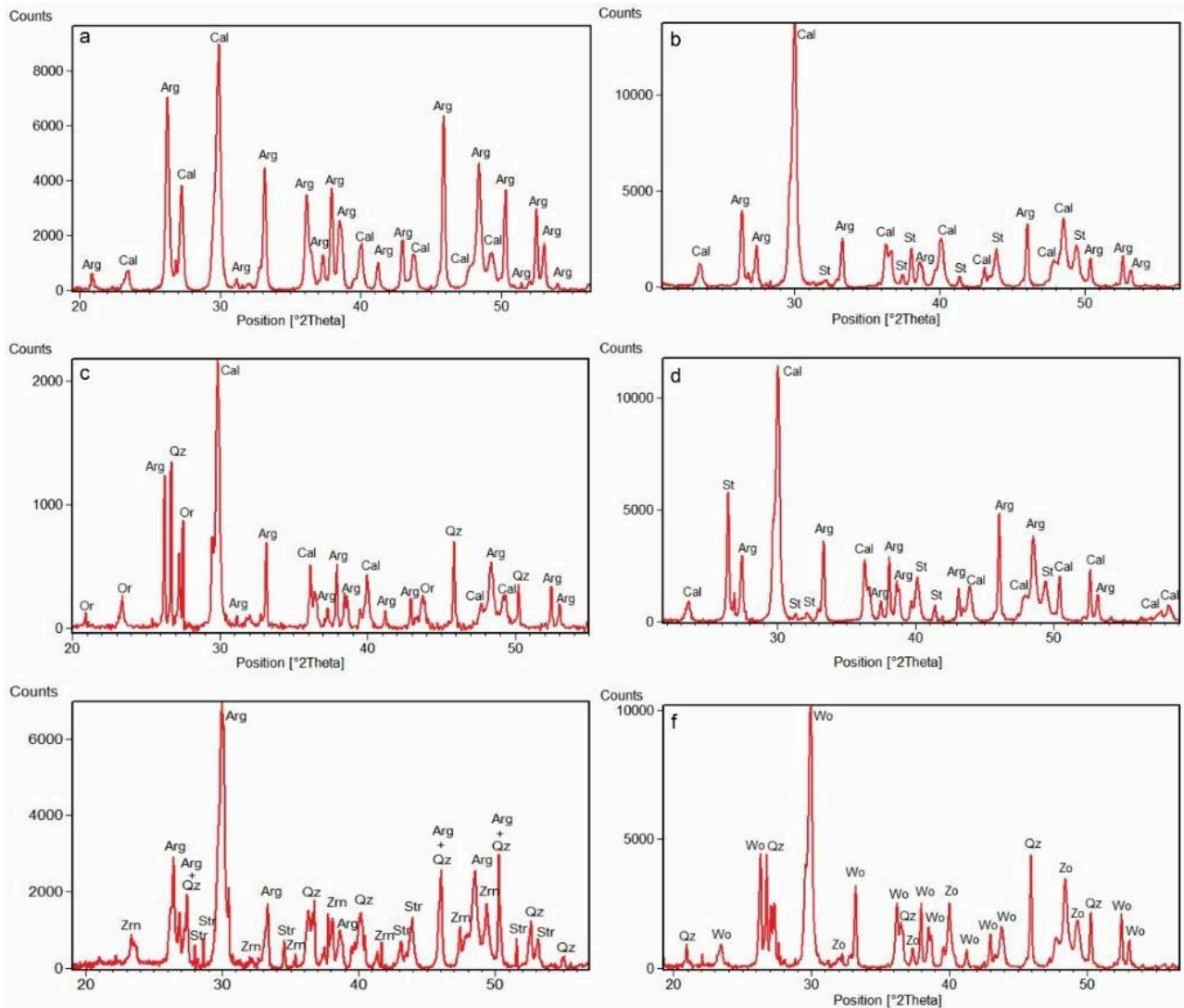


Figure 4 - X-ray diffractograms of the outer shelf sediment samples. a) sample 17 shows peaks calcite (Cal) and aragonite (Arg); b) sample 46 shows peaks calcite, aragonite and staurolite (St); c) sample 55 shows calcite, aragonite, quartz (Qz) and orthoclase (Oz); d) sample 71 shows peaks calcite, aragonite and staurolite; e) sample 78 shows quartz, aragonite, strontianite (Str) and zircon (Zr); f) sample 130 shows peak wollastonite (Wo), quartz and zoisite (Zo).

Fourteen samples underwent XRF analysis to quantify the elements, and the results indicated significant concentrations in ten elements (Table 3). The analysis of Pearson's correlation coefficient among the ten most common elements revealed an abundance of metals in the following order: Ca, Si, Al, Fe, Sr, Zr, K, Ti, Mg, S. Strong negative correlations were observed between Ca-Si ($r = -0.85513$), Ca-Al ($r = -0.83514$), Ca-K ($r = -0.83507$), Ca-Ti ($r = -0.71723$), Si-Mg ($r = -0.80235$), Si-S ($r = -0.84956$), Al-Sr ($r = -0.70659$), Al-S ($r = -0.79501$), Fe-Sr ($r = -0.77501$), Sr-Ti ($r = -0.83972$), Zr-Mg ($r = -0.78627$) and S-K ($r = -0.81606$). Very strong positive correlations were

identified between Ca-Mg ($r = 0.91502$), Si-Al ($r = 0.96516$), Si-K ($r = 0.97088$) and Al-K ($r = 0.92553$). However, Sr-Zr ($r = -0.12146$) had negative weak correlations and K-Zr ($r = 0.18539$) positive weak correlations. No statistically significant correlations were observed between Ca-Zr, Si-Zr, Al-Zr, Sr-Zr, Zr-K, K-Ti, Sr-Mg, and Zr-S concentrations (Table 3).

Punctual SEM-EDS analyses were conducted on benthic foraminifera shells, revealing the presence of metals in the following proportions: Cl > Cu > Al > Fe > Ca > Zn > Sr > Mg > K > Cr > Zr > Si > Ar > Ti (Table 4). The shells showed signs of corrosion due to chemical dissolution (Fig. 5).

Table 3 - Pearson's correlation among the more frequent chemical elements in the bottom sediments.

	Ca	Si	Al	Fe	Sr	Zr	K	Ti	Mg	S
Ca	1									
Si	-0.85513	1								
Al	-0.83514	0.96516	1							
Fe	-0.63109	0.8538	0.87286	1						
Sr	0.73205	-0.68632	-0.70659	-0.77501	1					
Zr	-0.35269	0.37957	0.41236	0.67801	-0.41587	1				
K	-0.83507	0.97088	0.92553	0.7614	-0.61934	0.18539	1			
Ti	-0.71723	0.69281	0.68593	0.89804	-0.83972	0.76983	0.59457	1		
Mg	0.91502	-0.80235	-0.69928	-0.63788	0.51377	-0.78627	-0.79395	-0.63113	1	
S	0.81715	-0.84956	-0.79501	-0.5862	0.55528	-0.12146	-0.81606	-0.60866	0.73032	1

Table 4 - Concentrations of the chemical elements present in the foraminifera shells *Amphistegina gibbosa* (17), *Archaias angulatus* (34), *Elphidium articulatum* (55), and *Archaias angulatus* (69).

Samples	Element	Weight%	Atomic%
17	Mg	1.42	1.76
	Al	11.80	13.17
	Si	0.68	0.73
	Cl	39.14	33.23
	Ar	2.14	1.62
	K	2.92	2.25
	Ti	1.78	1.12
	Fe	4.59	2.47
	Cu	14.19	6.72
	Sr	2.08	0.71
	Al	11.35	12.28
34	Si	1.84	1.91
	Cl	28.45	23.42
	Ca	5.54	4.03
	Ti	1.10	0.67
	Fe	6.44	3.37
	Ni	1.88	0.93
	Cu	6.56	3.01
	Zn	11.19	5.00
	Mg	2.00	2.60
	Al	5.44	6.36
	Si	1.63	1.83
55	Cl	50.60	45.02
	Ca	4.69	3.69
	Cr	2.62	1.59
	Fe	2.50	1.41
	Cu	5.94	2.95
	Zn	4.53	2.19
	Sr	2.04	0.73
	Zr	2.39	0.83
69	Al	36.56	29.94
	Si	3.73	2.93
	Cl	6.75	4.20
	Ca	3.16	1.74
	Mn	0.37	0.15

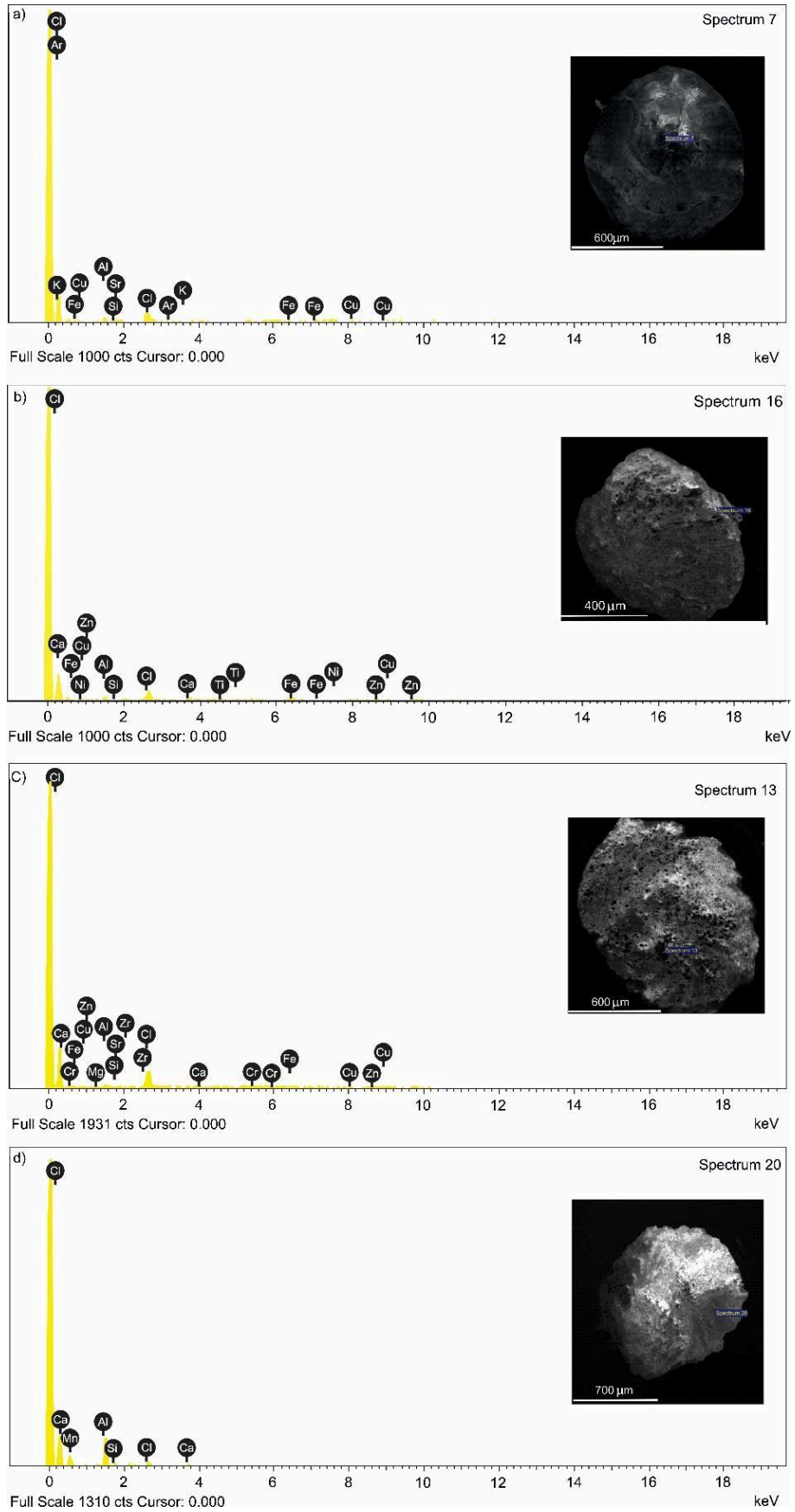


Figure 5 - Scanning Electron Microscopy images depicting composition of benthic foraminifera of the outer shelf sediments. *Amphistegina gibbosa* (sample 17) (a) displays Cl and Ar as the main elements in its dispersive energy spectra, while *Archaias angulatus* (sample 34) (b), *Elphidium articulatum* (sample 55) (c), and *Elphidium articulatum* (sample 69) (d) exhibit Cl as the major element in their dispersive energy spectra.

4.2 Statistical analysis

Cluster analysis depicted the relationship between metals and the content of organic matter and carbonate (Fig. 6). Group "A" consists of Ca and Si with a Euclidean distance of approximately 0.3. Group "B" is composed of S, Mg, and Sr, which exhibit similarities with values around 0.5. Group "C" is composed of K, Ti, Zr, Fe, and Al, with a similarity of approximately 0.6. Within this group, Fe and Al are the most similar, with values around 0.8.

Despite the distinct geochemical properties of Si and Ca, they reflect the co-occurrence patterns, a specific geochemical context, particularly in environments of mixed sediments in the study area, that influence their concentrations in the analyzed samples.

The largest factors in the multivariate PCA accounted for roughly 80% of the total variance (Fig.

7). The sediments are divided into two groups, with contrasting variances. The first group encompasses bioclastic and mixed sedimentary facies, all of which are intimately linked to Ca, Mg, Sr, S, CaCO₃, and Organic Matter. The second group consists of siliciclastic sediments, which show positive relationships between K, Si, and Al, and between Fe, Ti, and Zr (see PC2 in Fig. 7).

For instance, the K, Si, and Al elements are prevalent in sediments derived from continental sources rather than in carbonate sediments. Moreover, the Fe, Ti, and Zr suggest enrichment in heavy minerals typical of siliciclastic sediments. However, these elements exhibit more restricted variation among minerals, or with minor variance in relation to principal components (see PC1 in Fig. 7) representing an influence of carbonate environment. The positive and negative correlations observed in PC2 highlight distinct sources or processes of transport and deposition..

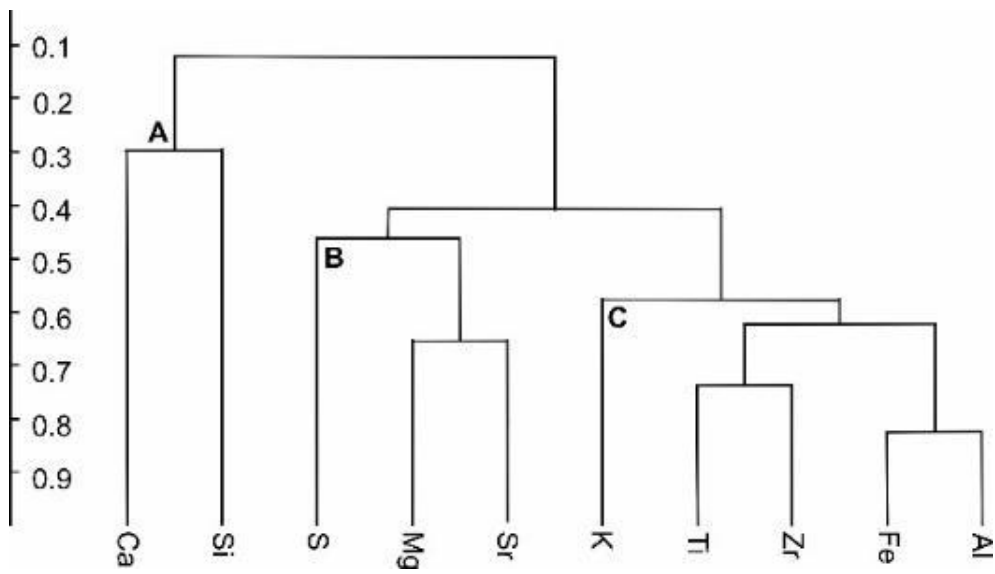


Figure 6 - Cluster analysis showing three groups of the major metals in the sedimentary sandy facies: bioclastic, biosiliciclastic, silicibioclastic, and siliciclastic.

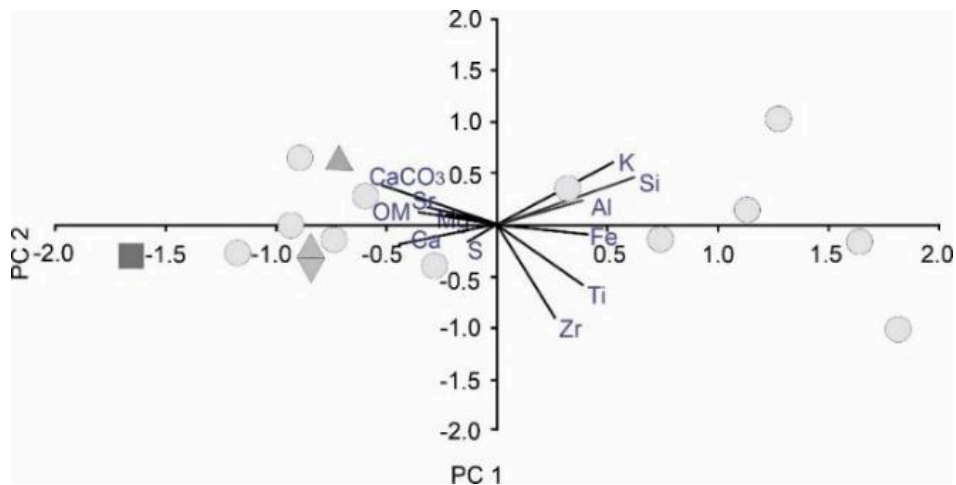


Figure 7 - Multivariate PCA analysis showing the geochemical affinity between metals, carbonate content, and organic matter in the sedimentary sandy facies: bioclastic (square symbol); biosiliciclastic (triangle); silicibioclastic (diamond); and siliciclastic (circle).

5. Discussion

5.1 Sediment Sources Signatures

This study employed tracers such as Si, Al, Fe, K, Ti, and Zr to identify continental sources, and used Ca, Sr, Mg, and S elements as indicators of marine sediments. The strong negative correlations between Ca and Si, Al, K, and Ti, as well as the Si-S, Fe-Sr, and Zr-Mg, highlight the differences in composition of continental and marine sediments (Table 3). According to the PCA analysis, the presence of bioclastic and mixed sedimentary facies is associated with elevated carbonate content, organic matter, and the elements Ca, Mg, Sr, and S (Fig. 7). As expected, high concentrations of Ca occur in the form of aragonite and calcite in marine carbonate sediments (Fig. 4; Table 4). The strong positive correlation between Ca-Mg, Ca-Sr, and Ca-S suggests in situ carbonate production, often associated with biological activity, organic matter, and origin in carbonate-rich environments. In contrast, the siliciclastic facies found on the outer continental shelf exhibit a strong positive correlation between Si-Al, Si-K, and Al-K. Hence, these positive correlations support the idea that carbonate and siliciclastic facies have distinct sources and depositional processes.

Most bioclastic sediments, constituted of Halimeda fragments, molluscs, coral algae, and benthic foraminifera, have high levels of Ca, Mg, and Sr. The Mg and Sr ions in seawater lead to the formation of aragonite (Sr-rich) and calcite (Mg-rich), which co-precipitated in a biogeochemical process (Martins et al. 2012, Cohen & McConnaughey 2003). The strong correlation between Ca and Mg result from an easy incorporation of Mg in calcite and aragonite in the calcareous shells of marine organisms indicating that metal scavenging processes and the metal-rich seawater influences the biomineralization (Ries 2005, Finch & Allison 2007). Similar to the study area, the neighborhood Ceará shelf is characterized by Sr-rich aragonite carbonate facies (Freire et al. 2004, Marques et al. 2008, Ximenes Neto et al. 2018), which sediment pattern extends northward to the equatorial continental shelf (e.g., Alfonso et al. 2006). Thus, the main factors determining the Ca, Mg, and Sr contents in the modern bioclastic facies are biological and physicochemical environmental interactions.

The presence of Si, Al, Zr, Ar, and Cr in the foraminifera shells observed in this study suggests the involvement of terrigenous particles, thereby reflecting secondary post-depositional processes (Fig. 5a). The structure of the calcareous benthic foraminifera, specifically *Amphistegina gibbosa* and *Elphidium articulatum*, was found to be influenced by the chemical elements found in seawater. For instance, in the Baltic Sea, several metals (i.g., Ca, Sr, Mg, Mn, Zn, Fe, and Cu) occur in shells of bivalve molluscs built with different calcium carbonate polymorphs (Lea 1999, Rainbow et al. 2004, Piwoni-Piórewicz et al. 2021). This influence was observed through reactions

and substitution of elements and producing a paragenesis mixing with biota (Reichart et al. 2003, Russell et al. 2004).

The mineralogical composition and the cluster analysis show that the siliciclastic facies indicators (high concentration of Si, Al, Fe, Zr, K, and Ti) have great similarity (Fig. 6) providing evidence of a common source. The siliciclastic sediments contain minerals of continental sources as quartz, orthoclase, staurolite, zoisite, wollastonite, and zircon (XRD analysis of samples 55, 71, 78, and 130 in Fig. 4). These results are consistent with previous studies (Silva & Vital 2000; Vital & Guedes 2000, Sousa et al. 2000), which identified a variety of translucent and opaque heavy minerals as hornblende, epidote, zircon, staurolite, kyanite, andalusite, tourmaline, titanite, anthophyllite, zoisite, rutile, garnet, cordierite, siderite, and sillimanite in the Açu river-delta and in the inner shelf. The neighborhood Ceará shelf also has similar siliciclastic sediment compositions formed by Fe, Al, Si, Mn, Cr, Zn, Ti, and K from predominantly continental sources (Aguiar Neto et al. 2014, Ximenes Neto et al. 2018), with minerals of ilmenite, tourmaline, epidote, hornblende, monazite, staurolite, sillimanite, rutile, magnetite, zircon, andalusite, kyanite, garnet (Cavalcanti et al. 1993), which are derived from the pre-Cambrian granites (Freire et al. 2004). The geochemical signature of siliciclastic facies along these continental shelves points to a common provenance resulting from the weathering of igneous and metamorphic sources.

The mineralogy of the siliciclastic sediments trapped in inter reef environments of the outer continental shelf (Fig. 4 and Table 3) is coherent with the lithology of the land areas surrounding the Açu and Apodi drainage basin. These land areas are predominantly of Neoproterozoic and Paleoproterozoic metamorphic basement terrains (gneisses and orthogneisses) and Cretaceous sandstones and calcareous rocks (Silva & Vital 2000). The study by Almeida et al. (2017) found zircon and rutile in the sediments, indicating their maturity and pointing to the fluvial systems as the main contributors to deposits on the continental slope and rise. Furthermore, the Açu and Apodi rivers were the only channels through which sediments from inner land sources reached the modern outer shelf region during Quaternary periods (Vital et al. 2010b; Gomes et al. 2016, 2020). Hence, the siliciclastic sediments found on the outer shelf originate from the innermost land and ultimately mix with reworked detrital marine sediments.

5.2 Controls on Modern and Relict Sedimentation

The siliciclastic and carbonate facies along the outer shelf have distinct statistical patterns and geochemical differences which allowed to access the marine and continental sources, as well as the deposition and mixing processes. For instance, the bioclastic facies were formed and deposited in situ,

while the trace elements present in the shells, the ages, and the state of preservation of the benthic foraminifera, indicate a post-depositional process (e.g., Alavi et al. 1989, Billups et al. 2022, Eichler et al. 2019, 2024). In contrast, the textural maturity of the siliciclastic sediments, especially the moderately sorting, provide evidences of intense transport and reworking (e.g., Pilkey et al. 1988, Nascimento Silva & Gomes 2019), which is incompatible with the modern hydrodynamics of the outer shelf environment (Damasceno et al. 2022). Further, siliciclastic deposits are located in patches within inter-reef formations, approximately 30 km from coastal terrigenous sources, and preserved due to low oceanographic energy in inter-reef areas, indicating their relict origin.

Considering the steep outer shelf gradient (1:200), the regional morphologies (i.e., terraces, reefs) (Gomes et al. 2020), and the higher energy conditions during marine transgression crossed this region (i.e., coastal wave, alongshore, and tidal currents), this morphological setting controlled the preservation of the terrigenous relicts and the mixing sedimentation process outside reef areas along the outer shelf. For example, relict sediments on the Turkey shelf occur patched on deeper parts of the shelf, as sea level reached approximately its present position nearly 5 kyr B.P., while the bulk of the siliciclastic input began to be deposited in the inner shelf zone (Alavi et al. 1989). In the study area, the last transgression allowed only a short depositional time (~11 to ~9 kyr), small horizontal (~8 km), and vertical space (between 25-70 m water depths) for deposition and preservation of terrigenous sediments. Besides, in this phase of the transgression, the recent submerged shelf provided favorable conditions to the development of the Açu reefs (Nascimento Silva et al. 2018), as they acted as traps for the terrigenous sediments carried by the rivers. The subsequent rising sea-level rapidly flooded the incised valleys, resulting in the landward migration of river-mouth deposits and the entrapment of relict sediments within the reef field.

These traps preserved the detrital sediments inside the Açu reef field, also in depressions of older relieves, from wave, tide, and currents, which were not able to completely remove the relict sediments. In contrast, there are no siliciclastic sediments within the Açu incised valley at its middle and outer portion (Gomes et al. 2015). According to local studies (Schwarzer et al. 2006; Lima and Vital, 2006; Vital et al., 2010b; Gomes et al., 2014, 2016), the Açu and Apodi Rivers incised the entirely exposed shelf during the Last Glacial Maximum. These river valleys bypassed sediments from land sources, loading the heavy minerals, to the shelf edge and to deep waters (Almeida et al. 2015, 2017). However, the valley is covered by surficial sediments, mainly carbonate muds, that are currently reworked by channelized tidal-flows (Gomes et al. 2016). Therefore, river and coastal sediments do not affect the modern outer shelf sedimentation and

consequently siliciclastic deposits are older than the sedimentation intervals that covered almost the entire outer shelf with carbonates.

The ages of the carbonate sediments are earlier than the maximum of 660 cal. BP (conventional ages 935 ± 30 BP and 715 ± 30 BP), which fall in the Late Holocene, when the sea level and coastline were already very near the present-day position (Barbosa et al. 2018). The last plenty interaction between river and coastal processes in the zone of the modern outer shelf was prior to 9 kyr, based on sea-level indicators at 20-25 m (Gomes et al. 2020). Further, the RN sea-level curves (Bezerra et al. 2003, Stattegger et al. 2006, Kumar et al. 2018) show that the coastline reached the present position after around 7 kyr entirely drowning the shelf. Thus, consistent with the position of the Açu reefs, between 25 and 55 m and detached 25 km far from the coast (Fig. 1), the inter reef siliciclastic deposits (Fig. 2) were isolated from land sources for at least since the Middle and Late Holocene.

There are noteworthy implications for carbonate depositional processes. Considering the last millennia, the dated carbonate sediments inside the reef field (samples Acu01 and Acu02) and also outside (samples Acu03 and Tub01) were not buried, and sediments were only reworked locally. Besides, geophysical high-resolution seismic data show that the open areas of the outer shelf have only a modest thickness of the Holocene sediment package with maximum 3 m (Gomes et al. 2014, Nascimento Silva et al. 2018). This indicates a poor carbonate production or a slow sedimentation rate. In contrast, recent studies conducted in the Açu reefs area support the idea that the outer shelf environment is favorable to benthic habitats due to factors such as reef and valley structures, water quality, temperature, and nutrient-rich upwelling (Roriva et al. 2019, Billups et al. 2022, Damasceno et al. 2022, Eichler et al. 2024). Despite this, the coeval outer shelf and reef environments display significant discrepancies in the spatial and timing of carbonate and siliciclastic deposits. The reef fields, specifically, have been subjected to a slow burial process since the Late Holocene to the present day.

6. Conclusions

The textural maturity and chemical contents of the carbonate and siliciclastic sedimentary facies are directly related to their marine and continental source, respectively. The elements Ca, Sr, Mg, and S are derived from marine sources and exhibit a negative correlation with Si, Al, and Zr, which are of continental origin. This contrast between marine and continental elements is clearly seen in the multivariate analysis, where two distinct groups are identified. The presence of major trace elements revealed that the siliciclastic facies come from terrigenous sediments in the Açu and Apodi rivers, transported during shelf exposure and trapped in the Açu inter-reef area.

By examining radio-carbon ages, geochemical analysis, and post-depositional chemical processes in foraminifera, it can be concluded that the carbonate sediments are from the late Holocene period and have low sedimentation rates. The siliciclastic sediments are older than the drowning of the shelf, which occurred prior to the Middle Holocene. Hydrodynamic incompatibility between the siliciclastic facies and carbonates leads to contrasting depositional processes. The relief and sediment texture of the outer shelf indicate that in the Early Holocene, the coasts experienced higher hydrodynamic energy compared to the present coastline. Sedimentation on the outer shelf is influenced by sea-level changes, fluvial input, shelf morphology, hydrodynamics, erosion, transport, and trapping. Siliciclastic sediments are present in protected areas of the reef fields, far from the coast, with limited preservation on the open outer shelf. Additional investigation is needed due to the challenge of punctuating lateral facies mixing in this outer shelf setting.

Acknowledgments

Thanks are due to the crew of the ship Comte. Manhães of the Brazilian Navy (SECIRM/SSN-3), the GGEMMA group for their support during the data acquisition, PPGG/UFRN, and laboratories of the Departments of Geology, Materials Engineering, and Chemistry for the provided academic infrastructure for this research. We also thank CAPES for funding the master's scholarship of the first author, and to CNPq for the research grant of the MPG (302375/2022-8) and HV (315742/2020-8). To the project CAPES Ciências do Mar II (23038.004320/2014-11). This is the scientific research of INCTAmbTropic–Brazilian National Institute of Science and Technology for Tropical Marine Environments (CNPq/FAPESB/CAPES).

Credit author statement

L.L.N.S.: Conceptualization, Formal Analysis, Investigation, Methodology, Visualization, Writing – original draft.

M.P.G.: Conceptualization, Data curation, Funding acquisition, Investigation, Methodology, Project administration, Supervision, Writing – review & editing.

P.E.P.B.: Methodology, Validation, Writing – review & editing.

H.V.: Resources, Validation, Writing – review & editing.

References

AGUIAR NETO J.E., DE LACERDA L.D., MIGUENS F.C., MARINS R.V. 2014. The geostatistics of the metal concentrations in sediments from the eastern Brazilian continental shelf in areas of gas and oil production. *Journal of South America Earth Sciences*, 51:91–104. <https://doi.org/10.1016/j.jsames.2013.12.005>

- ALAVI S.N., EDIGER V., ERGIN M. 1989. Recent sedimentation on the shelf and upper slope in the Bay of Anamur, southern coast of Turkey. *Marine Geology*, 89:29–56.
- ALFONSO J.A., MARTÍNEZ M., FLORES S., BENZO Z. 2006. Distribution of trace elements in offshore sediments of the Orinoco Delta. *Journal of Coastal Research*, 22:502–510. <https://doi.org/10.2112/03-0142.1>
- ALMEIDA N.M., VITAL H., GOMES M.P. 2015. Morphology of submarine canyons along the continental margin of the Potiguar Basin, NE Brazil. *Marine Petroleum Geology*, 68:307–324.
- ALMEIDA N., VITAL H., EICHLER P.P.B. 2017. Aspectos sedimentológicos do talude setentrional do Rio Grande do Norte, NE do Brasil. *Pesquisas em Geociências*, 44(3):537–554.
- ANGULO R.J., SOUZA M.C., ROSA M.L.C.C., CARON F., BARBOZA E.G., COSTA M.B.S.F., MACEDO E., VITAL H., GOMES M.P., GARCIA K.B. 2022. Paleo-sea levels, Late-Holocene evolution, and a new interpretation of the boulders at the Rocas Atoll, southwestern Equatorial Atlantic. *Marine Geology*, 447:106780.
- ARZ H.W., PÄTZOLD J., WEFER G. 1998. Correlated millennial-scale changes in surface hydrography and terrigenous sediment yield inferred from Last-Glacial marine deposits off northeastern Brazil. *Quaternary Research*, 50:157–166. <https://doi.org/10.1006/qres.1998.1992>
- BARBOSA M.E.F., BOSKI T., BEZERRA F.H.R., LIMA-FILHO F.P., GOMES M.P., PEREIRA L.C., MAIA R.P. 2018. Late Quaternary infilling of the Assu River embayment and related sea level changes in NE Brazil. *Marine Geology*, 405:23–37. <https://doi.org/10.1016/j.margeo.2018.07.014>
- BASTOS A.C., QUARESMA V.S., MARANGONI M.B., D'AGOSTINI D.P., BOURGUIGNON S.N., CETTO P.H., SILVA A.E., AMADO FILHO G.M., MOURA R.L., COLLINS M. 2015. Shelf morphology as an indicator of sedimentary regimes: a synthesis from a mixed siliciclastic-carbonate shelf on the Eastern Brazilian Margin. *Journal of South America Earth Sciences*, 63:125–136.
- BEZERRA F.H.R., BARRETO A.M.F., SUGUIO K. 2003. Holocene sea-level history on the Rio Grande do Norte State coast, Brazil. *Marine Geology*, 196(1):73–89.
- BOSENCE D. 2021. Carbonate Shorelines and Shelves, 2nd edition. In: ALDERTON D., ELIAS S.A. (eds) *Encyclopedia of Geology*, Elsevier Inc., 942-954p. <https://doi.org/10.1016/b978-0-12-409548-9.11848-2>
- BRONK RAMSEY C. 2009. Bayesian analysis of radiocarbon dates, *Radiocarbon*, 51:337–360.
- BILLUPS K., EICHLER P.P.B., RAVELO C., NASCIMENTO SILVA L.L., VITAL H., GOMES M.P. 2022. Stable isotopic variability in individual benthic foraminifera from the continental shelf of tropical Brazil. *Journal of Foraminiferal Research*, 52(4):212–228.
- CAMARGO J.M.R., ARAÚJO T.C.M., FERREIRA B.P., MAIDA M. 2015. Topographic features related to recent sea level history in a sediment-starved tropical shelf: Linking the past, present and future. *Regional Studies in Marine Sciences*, 2:203–211. <https://doi.org/10.1016/j.rsma.2015.10.009>
- CATTANEO A., STEEL R.J. 2003. Transgressive deposits: a review of their variability. *Earth-Science Review*, 62:187–228. doi:10.1016/s0012-8252(02)00134-4
- CAVALCANTI V.M.M., FREIRE G.S.S., GOMES D.F. 1993. Depósitos de minerais pesados de interesse econômico na plataforma continental interna leste do Estado do Ceará. *Revista de Geologia*, 6:75-91.
- COHEN A.L., MCCONNAUGHEY T.A. 2003. Geochemical perspectives on coral mineralization. *Rev. Mineralogy Geochemistry*, 54:151–187. <https://doi.org/10.2113/0540151>
- DAMASCENO U.M., CINTRA M.M., GOMES M.P., VITAL H. 2022. Interactions between the North Brazilian Undercurrent (NBUC) and the Southwest Atlantic Margin. Implications for Brazilian shelf-edge systems. *Regional Studies in Marine Science*, 54:102486. <https://doi.org/10.1016/j.rsma.2022.102486>
- DIAS G.T.M., FERRAZ C.B. 2004. SAG – Sistema de Análise Granulométrica. Manual do Usuário. Dept. Geologia-Lagemar/UFF. Access: <http://www.igeo.uff.br>
- DOMINGUEZ J.M.L., DA SILVA R.P., NUNES A.S., FREIRE A.F.M. 2013. The narrow, shallow, low-accommodation shelf of central Brazil: Sedimentology, evolution, and human uses.

- Geomorphology, 203:46–59. <https://doi.org/10.1016/j.geomorph.2013.07.004>
- EICHLER P.P.B., NASCIMENTO SILVA L.L., ANDRADE A.U., MARTINS J.F.O., FARIAS C.L.C., MOURA D.S., AMORIM A., MARINHO L., VITAL H., GOMES M.P. 2019. Organically enriched sediments and foraminiferal species from the Açú Reef, indicators of upwelling in NE Brazil? *Marine Geology*, 417:106016.
- EICHLER P.P.B., VITAL H., GOMES M.P. 2024. Marine sediments from mesophotic reefs as indicators of offshore vortex in the Açú reef (Northeast, Brazil). *Journal of Aquaculture & Marine Biology*, 13(1):1–7. DOI: 10.15406/jamb.2024.13.00389
- EMERY K.O. 1968. Relict sediments on continental shelves of the world. *AAPG Bulletin*, 52:445–464.
- FERREIRA A.L., VITAL H., STATTEGGER K., CALDAS L.H.O., GOMES M.P., PEREZ Y.A.R., AQUINO DA SILVA A.G. 2022. Seismic architecture of the tidal channel system of Galinhos, equatorial Atlantic, Brazil. *Marine Geology*, 443:106685.
- FREIRE G.S.S., GOMES D.F., LIMA S.F., MAIA L.P., LACERDA L.D. 2004. Geochemistry of Continental Shelf Sediments of the Ceará Coast, North-Eastern Brazil. In: Drude de Lacerda L., Santelli R.E., Duursma E.K., Abrão J.J. (eds) *Environmental Geochemistry in Tropical and Subtropical Environments*. Environmental Science. Springer, Berlin, Heidelberg, 365–377p. https://doi.org/10.1007/978-3-662-07060-4_26
- FINCH A.A., ALLISON N. 2007. Coordination of Sr and Mg in calcite and aragonite. *Mineralogical Magazine*, 71:539–552. <https://doi.org/10.1180/minmag.2007.071.5.539>
- GAO Y., LI Z., WANG N., LI R. 2019. Controlling factors and the paleoenvironmental significance of chemical elements in Holocene calcareous root tubes in the Alashan Desert, Northwest China. *Quaternary Research*, 91:149–162. <https://doi.org/10.1017/qua.2018.80>
- GISCHLER E. 2011. Carbonate Environments. In: REITNER J., THIEL V. (eds) *Encyclopedia of Geobiology*. Encyclopedia of Earth Sciences Series. Springer, Dordrecht, 238–261p. https://doi.org/10.1007/978-1-4020-9212-1_49
- GOMES M.P., VITAL H. 2010. Revisão da compartimentação geomorfológica da Plataforma Continental Norte do Rio Grande do Norte, Brasil. *Revista Brasileira de Geociências*, 40(3):321–329.
- GOMES M.P., VITAL H., BEZERRA F.H.R., DE CASTRO D.L., MACEDO J.W.D.P. 2014. The interplay between structural inheritance and morphology in the equatorial Continental Shelf of Brazil. *Marine Geology*, 355:150–161.
- GOMES M.P., VITAL H., EICHLER P.P.B., GUPTA, B.K.S. 2015. The investigation of a mixed carbonate-siliciclastic shelf, NE Brazil: side-scan sonar imagery, underwater photography, and surface-sediment data. *Italian Journal of Geosciences*, 134(1):9–22.
- GOMES M.P., VITAL H., STATTEGGER K., SCHWARZER K. 2016. Bedrock control on the Assu Incised Valley morphology and sedimentation in the Brazilian equatorial Shelf. *International Journal of Sediment Research*, 31(2):181–193.
- GOMES M.P., VITAL H., DROXLER A.W. 2020. Terraces, reefs, and valleys along the Brazil northeast outer shelf: deglacial sea-level archives? *Geo-Marine Letters*, 40:699–711. <https://doi.org/10.1007/s00367-020-00666-4>
- GONZALEZ R., DIAS J.M.A., LOBO F., MENDES I. 2004. Sedimentological and paleoenvironmental characterization of transgressive sediments on the Guadiana Shelf (Northern Gulf of Cadiz, SW Iberia). *Quaternary International*, 120:133–144. <https://doi.org/10.1016/j.quaint.2004.01.012>
- HAMMER Ø., HARPER D.A.T., RYAN P.D. 2001. PAST: paleontological statistics software package for education and data analysis. *Palaeontologia Electronica*, 4:1–9.
- HEATON T.J., KÖHLER P., BUTZIN M., BARD E., REIMER R.W., AUSTIN W.E.N., BRONK RAMSEY C., GROOTES P.M., HUGHEN K.A., KROMER B., REIMER P.J., ADKINS J., BURKE A., COOK M.S., OLSEN J., SKINNER L.C. 2020. Marine20-the marine radiocarbon age calibration curve (0-55,000 cal. BP). *Radiocarbon*, 62(4):779–820. <https://doi.org/10.1017/RDC.2020.68>
- JORRY S.J., DROXLER A.W., MALLARINO G., DICKENS G.R., BENTLEY S.J., BEAUFORT L., PETERSON L.C., OPDYKE B.N. 2008. Bundled turbidite deposition in the central Pandora Trough (Gulf of Papua) since Last Glacial Maximum: Linking sediment nature and accumulation to sea level fluctuations at millennial timescale. *Journal of Geophysical Research Earth Surface*, 113:F01S19. <https://doi.org/10.1029/2006JF000649>
- KNOPPERS B., EKAU W., FIGUEIREDO A.G. 1999. The coast and shelf of East and Northeast Brazil and material transport. *Geo-Marine Letters*, 19(3):171–178.
- KUMAR M., BOSKI T., LIMA-FILHO F.P., BEZERRA F.H.R., GONZALEZ-VILA F.J., GONZALEZ-PEREZ J.A. 2018. Environmental changes recorded in the Holocene sedimentary infill of a tropical estuary. *Quaternary International*, 476:34–45.
- LARSONNEUR C. 1977. La cartographie des dépôts meubles sur le plateau continental français: méthode mise au point et utilisée en Manche *Journal de Recherche Océanographique*, 2:34–39.
- LEA D.W. 1999. Trace elements in foraminiferal calcite. In: SEN GUPTA B.K. (ed) *Modern Foraminifera*, Kluwer Academic Publishers, Great Britain, 259–277p. https://doi.org/10.1007/0-306-48104-9_15
- LIMA S.F., VITAL H. 2006. Geomorphological and paleogeographic characterization of continental shelf of the Apodi-Mossoró River, RN-Brazil. In: BREBBIA C.A. (ed) *Environmental problems in coastal regions VI: including oil spill studies*. Wessex Institut of Technology, Cambridge Printing, 351–360p.
- MARQUES W.S., SIAL A.N., DE ALBUQUERQUE MENOR E., FERREIRA V.P., SA FREIRE G.S., DE ALBUQUERQUE MEDEIROS LIMA E., BELO DE SOUZA R.L. 2008. Ancient coastlines in the continental shelf of the state of Ceará, northeast Brazil: Evidence from sediment chemistry and stable isotopes. *International Geology Review*, 50:1141–1156. <https://doi.org/10.2747/0020-6814.50.12.1141>
- MARTINS R., AZEVEDO M.R., MAMEDE R., SOUSA B., FREITAS R., ROCHA F., QUINTINO V., RODRIGUES A.M. 2012. Sedimentary and geochemical characterization and provenance of the Portuguese continental shelf soft-bottom sediments. *Journal of Marine Systems*, 91:41–52. <https://doi.org/10.1016/j.jmarsys.2011.09.011>
- MILLER, K.G., BROWNING, J.V., MOUNTAIN, G.S., SHERIDAN, R.E., SUGARMAN, P.J., GLENN, S., CHRISTENSEN, B.A., 2014. History of continental shelf and slope sedimentation on the US middle atlantic margin. *Geological Society Memoirs*, 41:21–34. <https://doi.org/10.1144/M41.3>
- MORAIS J.O., XIMENES NETO A.R., PESSOA P.R.S., DE SOUZA PINHEIRO L., 2020. Morphological and sedimentary patterns of a semi-arid shelf, Northeast Brazil. *Geo-Marine Letters*, 40:835–842. <https://doi.org/10.1007/s00367-019-00587-x>
- MOREIRA D.A., GOMES M.P., VITAL H. 2020. Shallow sedimentation of Natal shelf and coastal erosion implications, NE Brazil. *Geo-Marine Letters*, 40:843–851. <https://doi.org/10.1007/s00367-019-00594-y>
- MOUNT J.F. 1984. Mixing of siliciclastic and carbonate sediments in shallow shelf environments. *Geology*, 12(7):432–435.
- NASCIMENTO SILVA L.L., GOMES M.P. 2019. Statistical approach on mixed carbonate-siliciclastic sediments of the NE Brazilian outer shelf. *Geo-Mar Letters*, 39(165):1–13. <https://doi.org/10.1007/s00367-019-00625-8>
- NASCIMENTO SILVA L.L., GOMES M.P., VITAL H. 2018. The Açú reef morphology, distribution, and inter-reef sedimentation on the outer shelf of the NE Brazil equatorial margin. *Continental Shelf Research*, 160:10–22.
- NASCIMENTO NETO F.C., VITAL H., ARAÚJO I.R.F., GOMES M.P. 2019. Sand ridges field in the north inner shelf of Rio Grande do Norte, adjacent to Galinhos-Guamaré, Brazil. *Anuário do Instituto de Geociências*, 42(2):50–58.
- NISHA V., ACHYUTHAN H. 2014. Geochemical evaluation of sea surface sediments along the continental shelf, south east coast of India. *Indian Journal of Marine Sciences*, 43:241–251.
- PESSOA NETO O.D.C. 2003. Estratigrafia de sequências da plataforma mista neogênica na Baía Potiguar, Margem equatorial brasileira. *Revista Brasileira de Geociências*, 33(3):263–278.
- PILKEY O. H., BUSH D.M., RODRIGUEZ R.W. 1988. Carbonate-Terrigenous Sedimentation on the North Puerto Rico Shelf. In: DOYLE L.J., ROBERTS H.H. (eds) *Carbonate –*

- Clastic Transitions, Elsevier Science Publishers, Netherlands, 231–250p.
- PIWONI-PIÓREWICZ A., STREKOPYTOV S., HUMPHREYS-WILLIAMS E., KUKLIŃSKI P. 2021. The patterns of elemental concentration (Ca, Na, Sr, Mg, Mn, Ba, Cu, Pb, V, Y, U and Cd) in shells of invertebrates representing different CaCO₃ polymorphs: A case study from the brackish Gulf of Gdańsk (the Baltic Sea). *Biogeosciences*, 18:707–728. <https://doi.org/10.5194/bg-18-707-2021>
- RAINBOW P.S., FIALKOWSKI W., SOKOŁOWSKI A., SMITH B.D., WOŁOWICZ M. 2004. Geographical and seasonal variation of trace metal bioavailabilities in the Gulf of Gdansk, Baltic Sea using mussels (*Mytilus trossulus*) and barnacles (*Balanus improvisus*) as biomonitors. *Marine Biology*, 144:271–286. <https://doi.org/10.1007/s00227-003-1197-2>
- REICHART G.J., JORISSEN F., ANSCHUTZ P., MASON P.R.D. 2003. Single foraminiferal test chemistry records the marine environment. *Geology*, 31:355–358. [https://doi.org/10.1130/0091-7613\(2003\)031<0355:SFTCRT>2.0.CO;2](https://doi.org/10.1130/0091-7613(2003)031<0355:SFTCRT>2.0.CO;2)
- RIES J.B. 2005. Aragonite production in calcite seas: effect of seawater Mg/Ca ratio on the calcification and growth of the calcareous alga *Penicillus capitatus*. *Paleobiology*, 31:445–458. [https://doi.org/10.1666/0094-8373\(2005\)031\[0445:apicse\]2.0.co;2](https://doi.org/10.1666/0094-8373(2005)031[0445:apicse]2.0.co;2)
- ROVIRA D.P.T., GOMES M.P., LONGO G.O. 2019. Underwater valley at the continental shelf structures benthic and fish assemblages of biogenic reefs. *Estuarine, Coastal and Shelf Science* 224:245–252. <https://doi.org/10.1016/j.ecss.2019.05.001>
- RUSSELL A.D., HÖNISCH, B., SPERO H.J., LEA D.W. 2004. Effects of seawater carbonate ion concentration and temperature on shell U, Mg, and Sr in cultured planktonic foraminifera. *Geochimica et Cosmochimica Acta*, 68:4347–4361.
- SCHWARZER K., STATTEGGER K., VITAL H., BECKER M. 2006. Holocene coastal evolution of the Rio Açu Area (Rio Grande do Norte, Brazil). *Journal of Coastal Research*, 39:141–145.
- SEVASTJANOVA I., HALL R., ALDERTON D. 2012. A detrital heavy mineral viewpoint on sediment provenance and tropical weathering in SE Asia. *Sedimentary Geology*, 280:179–194. <https://doi.org/10.1016/j.sedgeo.2012.03.007>
- SILVA M.G., VITAL H., 2000. Provenance of Heavy-Minerals in the Piranhas-Açu River, Northeastern Brazil. *Revista Brasileira de Geociências*, 30:453–456. <https://doi.org/10.25249/0375-7536.2000303453456>
- SOUSA D.D.C., VITAL H., FONSECA V.P. 2000. Stratigraphic Significance of Heavy Minerals in Sediments of the Northeastern Brazil. *Revista Brasileira de Geociências*, 30:470–473. <https://doi.org/10.25249/0375-7536.2000303470473>
- STATTEGGER K., CALDAS L.H.O., VITAL H. 2006. Holocene coastal evolution of the Northern Rio Grande do Norte coast, NE, Brazil. *Journal of Coastal Research*, 39:151–156.
- TESTA V., BOSENCE D.W.J. 1999. Biological and physical control on the bedform generation in the Rio Grande do Norte inner shelf, Brazil. *Sedimentology*, 46:279–301.
- TUCKER M.E. 1985. Shallow-marine carbonate facies and facies models. In: Brenchley P.J., Williams B.P.J. (eds) *Sedimentology: Recent Developments and Applied Aspects*, 18:147–169. <https://doi.org/10.1144/gsl.sp.1985.018.01.08>
- VIEIRA F.V., BASTOS A.C., QUARESMA V.S., LEITE M.D., COSTA A., OLIVEIRA K.S.S., DALVI C.F., BAHIA R.G., HOLZ V.L., MOURA R.L., AMADO FILHO G.M. 2019. Along-shelf changes in mixed carbonate-siliciclastic sedimentation patterns. *Continental Shelf Research*, 187:103964. <https://doi.org/10.1016/j.csr.2019.103964>
- VITAL H., GUEDES I.M.G. 2000. Heavy Minerals of the Inner Continental Shelf Offshore the Açu River'S Delta (Northeastern Brazil). *Revista Brasileira de Geociências*, 30:457–459. <https://doi.org/10.25249/0375-7536.2000303457459>
- VITAL H., STATTEGGER K., AMARO V.E., SCHWARZER K., FRAZAO E.P., TABOSA W.F., SILVEIRA I.M. 2008. A modern high-energy siliciclastic-carbonate platform: continental shelf adjacent to Northern Rio Grande do Norte state, Northeastern Brazil. In: HAMPSON G.J., STEEL R.J., BURGESS P.M., DALRYMPLE R.W. (eds) *Recent Advances in Models of Siliciclastic Shallow-marine Stratigraphy* 90. SEPM Special Publication, 177–190p.
- VITAL H. 2009. The mesotidal barriers of Rio Grande do Norte. In: DILLENBURG S., HESP P. (eds) *Geology of Brazilian Holocene coastal barriers*. Springer-Verlag, Heidelberg, 289–324p.
- VITAL H., GOMES M.P., TABOSA W.F., FRAZÃO E.P., SANTOS C.L.A., PLÁCIDO JUNIOR J.S. 2010a. Characterization of the Brazilian Continental Shelf adjacent to Rio Grande do Norte State, NE Brazil. *Brazilian Journal of Oceanography*, 58(1):43–54.
- VITAL H., FURTADO S.F.L., GOMES M.P. 2010b. Response of Apodi Mossoró estuary-incised valley system (NE Brazil) to sea-level fluctuations. *Brazilian Journal of Oceanography*, 58(2):13–24.
- XIMENES NETO A.R., MORAIS J.O., CIARLINI C. 2018. Modern and relict sedimentary systems of the semi-arid continental shelf in NE Brazil. *Journal of South America Earth Sciences*, 84:56–68. <https://doi.org/10.1016/j.jsames.2018.03.004>
- WU L., MEI L., LIU Y., LUO J., MIN C., LU S., LI M., GUO L. 2017. Multiple provenance of rift sediments in the composite basin-mountain system: Constraints from detrital zircon U-Pb geochronology and heavy minerals of the early Eocene Jiangnan Basin, central China. *Sedimentary Geology*, 349:46–61. <https://doi.org/10.1016/j.sedgeo.2016.12.003>